

Comparison of thermal lensing effects between single-end and double-end diffusion-bonded Nd:YVO₄ crystals for ${}^4F_{3/2} \rightarrow {}^4I_{11/2}$ and ${}^4F_{3/2} \rightarrow {}^4I_{13/2}$ transitions

Y. T. Chang, Y. P. Huang, K. W. Su*, and Y. F. Chen

Department of Electrophysics, National Chiao Tung University, Hsinchu, Taiwan

*Corresponding author: sukuanwei@mail.nctu.edu.tw

Abstract: The effective focal lengths of thermal lens in diode-end-pumped continuous-wave Nd:YVO₄ lasers for the ${}^4F_{3/2} \rightarrow {}^4I_{11/2}$ and ${}^4F_{3/2} \rightarrow {}^4I_{13/2}$ transitions were determined. The experimental results revealed that the thermal lensing effect for the ${}^4F_{3/2} \rightarrow {}^4I_{11/2}$ transition can be sufficiently improved by employing a single-end diffusion-bonded Nd:YVO₄ crystal replacing a conventional Nd:YVO₄ crystal. However, using a double-end diffusion-bonded Nd:YVO₄ crystal was a great improvement over a single-end diffusion-bonded Nd:YVO₄ crystal for the ${}^4F_{3/2} \rightarrow {}^4I_{13/2}$ transition with stronger thermal lensing effect.

©2008 Optical Society of America

OCIS codes: (140.3480) Lasers, diode-pumped; (140.6810) Thermal effects.

References and links

1. T. Y. Fan and R. L. Byer, "Diode laser-pumped solid-state lasers," *IEEE J. Quantum Electron.* **24**, 895-912 (1988).
2. A. K. Cousins, "Temperature and thermal stress scaling in finite-length end-pumped laser rods," *IEEE J. Quantum Electron.* **28**, 1057-1069 (1992).
3. W. Koechner, *Solid-State Laser Engineering*, 6th ed. (Springer, New York, 2006), Chap. 7.
4. Y. F. Chen, "Design criteria for concentration optimization in scaling diode end-pumped lasers to high powers: influence of thermal fracture," *IEEE J. Quantum Electron.* **35**, 234-239 (1999).
5. Y. F. Chen, T. M. Huang, C. F. Kao, C. L. Wang, and S. C. Wang, "Optimization in scaling fiber-coupled laser-diode end-pumped lasers to higher power: influence of thermal effect," *IEEE J. Quantum Electron.* **33**, 1424-1429 (1997).
6. Y. F. Chen, C. F. Kao, T. M. Huang, C. L. Wang, and S. C. Wang, "Influence of thermal effect on output power optimization in fiber-coupled laser-diode end-pumped lasers," *IEEE J. Sel. Top. Quantum Electron.* **3**, 29-34 (1997).
7. W. A. Clarkson, "Thermal effects and their mitigation in end-pumped solid-state lasers," *J. Phys. D* **34**, 2381-2395 (2001).
8. S. C. Tidwell, J. F. Seamans, M. S. Bowers, and A. K. Cousins, "Scaling CW diode-end-pumped Nd:YAG lasers to high average powers," *IEEE J. Quantum Electron.* **28**, 997-1009 (1992).
9. B. Neuenschwander, R. Weber, and H. P. Weber, "Determination of the thermal lens in solid-state lasers with stable cavities," *IEEE J. Quantum Electron.* **31**, 1082-1087 (1995).
10. B. Ozygus, and Q. Zhang, "Thermal lens determination of end-pumped solid-state lasers using primary degeneration modes," *Appl. Phys. Lett.* **71**, 2590-2592 (1997).
11. F. Song, C. Zhang, X. Ding, J. J. Xu, and G. Y. Zhang, "Determination of thermal focal length and pumping radius in gain medium in laser-diode-pumped Nd:YVO₄ lasers," *Appl. Phys. Lett.* **81**, 2145-2147 (2002).
12. S. Chénais, S. Forget, F. Druon, F. Balembois, and P. Georges, "Direct and absolute temperature mapping and heat transfer measurements in diode-end-pumped Yb:YAG," *Appl. Phys. B* **79**, 221-224 (2004).
13. S. Z. Fan, X. Y. Zhang, Q. P. Wang, S. T. Li, S. H. Ding, and F. F. Su, "More precise determination of thermal lens focal length for end-pumped solid-state lasers," *Opt. Commun.* **266**, 620-626 (2006).
14. F. Hanson, "Improved laser performance at 946 and 473 nm from a composite Nd:Y₃Al₅O₁₂ rod," *Appl. Phys. Lett.* **66**, 3549-3551 (1995).
15. R. Weber, B. Neuenschwander, M. M. Donald, M. B. Roos, and H. P. Weber, "Cooling schemes for longitudinally diode laser-pumped Nd:YAG rods," *IEEE J. Quantum Electron.* **34**, 1046-1053 (1998).

16. M. Tsunekane, N. Taguchi, T. Kasamatsu, and H. Inaba, "Analytical and experimental studies on the characteristics of composite solid-state laser rods in diode-end-pumped geometry," *IEEE J. Sel. Top. Quantum Electron.* **3**, 9-18 (1997).
17. M. Tsunekane, N. Taguchi, and H. Inaba, "Efficient 946-nm laser operation of a composite Nd:YAG rod with undoped ends," *Appl. Opt.* **37**, 5713-5719 (1998).
18. M. Tsunekane, N. Taguchi, and H. Inaba, "Improvement of thermal effects in a diode-end-pumped, composite Tm:YAG rod with undoped ends," *Appl. Opt.* **38**, 1788-1791 (1999).
19. M. P. MacDonald, Th. Graf, J. E. Balmer, and H. P. Weber, "Reducing thermal lensing in diode-pumped laser rods," *Opt. Commun.* **178**, 383-393 (2000).
20. J. Šulc, H. Jelínková, V. Kubeček, K. Nejezchleb, and K. Blažek, "Comparison of different composite Nd:YAG rods thermal properties under diode pumping," *Proc. SPIE* **4630**, 128-134 (2002).
21. D. Kracht, R. Wilhelm, M. Frede, K. Dupré, and L. Ackermann, "407 W end-pumped multi-segmented Nd:YAG laser," *Opt. Express* **13**, 10140-10144 (2005), <http://www.opticsinfobase.org/oe/abstract.cfm?URI=oe-13-25-10140>.
22. Z. Zhuo, T. Li, X. Li, and H. Yang, "Investigation of Nd:YVO₄/YVO₄ composite crystal and its laser performance pumped by a fiber coupled diode laser," *Opt. Commun.* **274**, 176-181 (2007).
23. Y. F. Chen, "Pump-to-mode size ratio dependence of thermal loading in diode-end-pumped solid-state lasers," *J. Opt. Soc. Am. B* **17**, 1835-1840 (2000).
24. M. E. Innocenzi, H. T. Yura, C. L. Fincher, and R. A. Fields, "Thermal modeling of continuous-wave end-pumped solid-state lasers," *Appl. Phys. Lett.* **56**, 1831-1833 (1990).
25. W. Koechner, "Thermal lensing in a Nd:YAG laser rod," *Appl. Opt.* **9**, 2548-2553 (1970).

1. Introduction

Diode-pumped solid-state laser has been adopted widely due to its compactness, high efficiency, and reliability [1]. Comparing with a diode-side-pumped configuration, the smaller laser beam waist, higher density of pump power, and inhomogeneous heating make thermal lensing effect become a serious problem in a diode-end-pumped configuration. The localized absorption of pump power in a laser crystal leads heat converted from pump power to accumulate near the pumped facet of laser crystal. The nonuniform temperature distribution of laser crystal is represented by a parabolic-logarithmic function [2]. The temperature-dependent variation of refractive index and the end bulging effect make laser crystal act as a thermal lens [3]. Owing to the nonuniform temperature distribution the temperature gradients accrue stress that could bring thermal fracture under high pump power operation [3]. There exists a fracture-limited pump power for laser crystal that makes scaling to a higher average power be restricted [4]. For a diode-end-pumped solid-state laser, the laser performance including laser stability, maximum achievable average power, efficiency, and degradation of laser beam quality is significantly influenced by thermal lensing effect [5-7]. Therefore, promotion of laser performance can be accomplished by efficient reduction of thermal lensing effect. End-pumped solid state laser cavity can be designed to optimize the laser performance by determining the focal length of thermal lens. Several methods for determining the focal length of thermal lens in diode-end-pumped laser crystal have been presented [8-13]. In the past few years, employing a composite crystal with nonabsorbing undoped end has been regarded as a promising method for cooling the laser crystal to improve the laser performance of diode-pumped solid state laser [14-22]. With the reduction of temperature and stress, a more uniform longitudinal temperature distribution can be generated to bring out a higher fracture-limited pump power and a higher average power.

Nd:YVO₄ crystal has been seen as an excellent laser material for diode-pumped solid-state laser due to its broad absorption bandwidth and large laser emission cross section at the ⁴F_{3/2}→⁴I_{11/2} (1064 nm) and ⁴F_{3/2}→⁴I_{13/2} (1342 nm) transitions. In this work, we measured the focal lengths of thermal lens for one conventional and two types of composite Nd:YVO₄ crystal, and for the 1064- and 1342-nm transitions. One composite Nd:YVO₄ crystal is bounded with an undoped end at its pumped facet, and the other composite crystal is bounded with undoped ends at its two facets. The composite crystals were fabricated by the method of diffusion-bonding with high quality on the interface. The simple setup of continuous-wave (CW) laser was utilized to measure the focal length of thermal lens under easy operation. While the cavity length was increased to the critical cavity length, the thermal lensing effect led the laser cavity to become unstable. By finding the critical cavity length, the effective

focal length of thermal lens can be worked out. We observed that the stronger thermal lensing effect in Nd:YVO₄ crystal for the 1342-nm transition than that for the 1064-nm transition due to the higher thermal loading accompanying the lower conversion efficiency. The power performance, focal lengths of thermal lens and thermal lensing effects for the three types of Nd:YVO₄ crystal for the 1064 and 1342 nm transitions will be discussed in this work.

2. Experimental setup

The experimental setup shown in Fig. 1 for measuring effective focal lengths of thermal lens in a diode-end-pumped laser crystal is the setup of normal CW Nd:YVO₄ laser. The output coupler connected with a stepper motor can be moved in the longitudinal direction to change the cavity length. The cavity length can be changed from 2.5 to 50 cm by controlling the stepper motor. The laser crystal was pumped by an 808-nm fiber-coupled laser diode with a core diameter of 0.8 mm, a numerical aperture of 0.16, and the maximum output power was 22 W. The pump beam was reimaged into the laser crystal and the radius was about 0.4 mm. The laser crystal was wrapped in indium foil and mounted on water-cooled copper blocks. The water temperature was maintained at 17°C. The entrance face of the 500-mm radius-of-curvature concave front mirror was coated for antireflection at the pump wavelength of 808nm ($R < 0.2\%$) and the other face was coated for high-transmission at 808 nm ($T > 90\%$) as well as high-reflection ($R > 99.8\%$) at the lasing wavelength. In this work, we consider the thermal lensing effect for the diode-end-pumped CW Nd:YVO₄ lasers operated at 1064 and 1342 nm. The individual coatings of front mirrors and output couplers were required for achievement of different lasing wavelengths. The two flat output couplers had the reflectance of 88% at 1064 and 92% at 1342 nm used for CW 1064 and 1342 nm lasers, respectively.

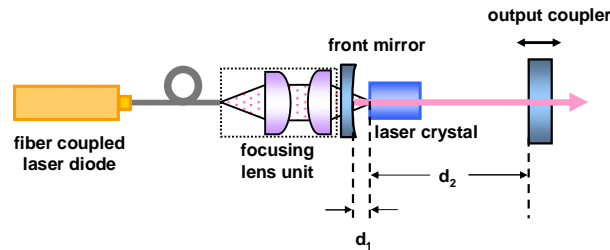


Fig. 1. Experimental setup of a diode-end-pumped Nd:YVO₄ CW laser for measuring the effective focal length of thermal lens in the laser crystal.

Figure 2 shows the three types of a-cut Nd:YVO₄ laser crystal employed in this work. Fig. 2(a) shows a 3 mm × 3 mm × 9 mm, 0.27-at.% Nd:YVO₄ crystal. Fig. 2(b) shows a 4 mm × 4 mm × 12 mm diffusion-bonded crystal called YVO₄-Nd:YVO₄ with single 2.7-mm-long undoped YVO₄ end at the pumped facet of 0.3-at.% active Nd:YVO₄ crystal. Fig. 2(c) shows a 4 mm × 4 mm × 14 mm diffusion-bonded crystal called YVO₄-Nd:YVO₄-YVO₄ with double 2.1-mm-long undoped YVO₄ end bonded to the both facets of 0.3-at.% active Nd:YVO₄ crystal. The Nd concentration was measured by the company supplying the crystals. Both sides of the three crystals were coated for antireflection at 1064 and 1342 nm ($R < 0.2\%$).

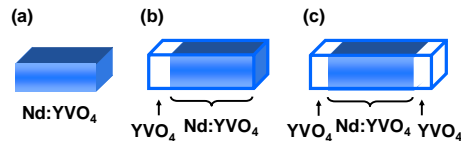


Fig. 2. The three types of laser crystal with different structures. (a) Conventional Nd:YVO₄ crystal. (b) Diffusion-bonded Nd:YVO₄ crystal with single-end at its pumped facet (YVO₄-Nd:YVO₄). (c) Diffusion-bonded Nd:YVO₄ crystal with double-end (YVO₄-Nd:YVO₄-YVO₄).

3. Experimental results and discussions

The laser performance of diode-end-pumped solid-state laser was strongly affected by thermal lensing effect. Figure 3 and Fig. 4 depict experimentally measured average CW power of 1064 and 1342 nm with respect to the cavity length for the three types of Nd:YVO₄ crystal under individual pump power, respectively. The sign of P_{in} in the Fig. 3 and Fig. 4 means the input pump power. The average CW power was optimized at the cavity length of 2.5 cm with pump power of 8.32 and 7.61 W for 1064 and 1342 nm, respectively. In order to make sure that the transverse mode was the TEM₀₀ mode without high-order mode, the optimization was done near the pump threshold. Note that while the cavity length was increased and the power was decreased rapidly, optimizing average power was not allowed. It is because the extraordinary high-order mode may compensate the power decay from thermal lensing effect.

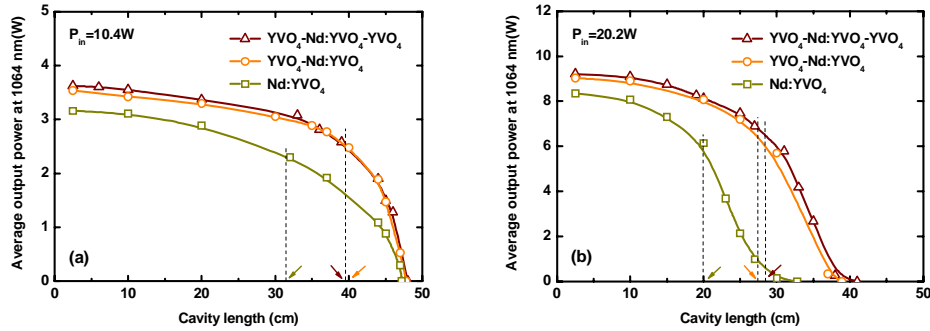


Fig. 3. Experimentally measured average CW output power of 1064 nm with respect to the cavity length for the three types of Nd:YVO₄ laser crystal with an input pump power (a) P_{in}=10.4W (b) P_{in}=20.2W. The arrows indicate the locations of critical cavity length.

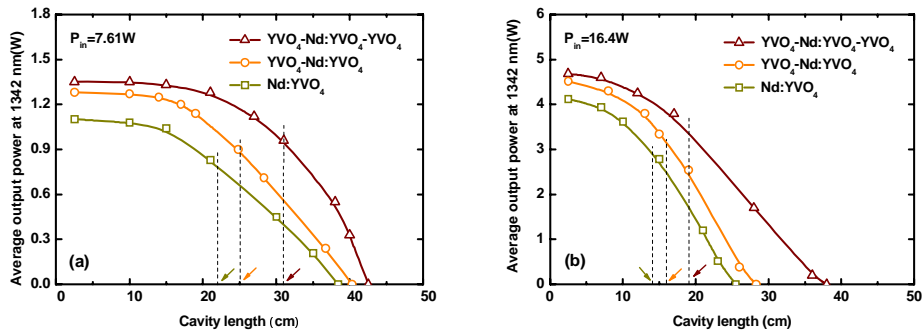


Fig. 4. Experimentally measured average CW output power of 1342 nm with respect to the cavity length for the three types of Nd:YVO₄ laser crystal with an input pump power (a) P_{in}=7.61W (b) P_{in}=16.4W. The arrows indicate the locations of critical cavity length.

While the cavity length was increased to a critical cavity length, the strong thermal lensing effect caused the laser cavity to become unstable. The relationships between average CW output power and cavity length are shown as Fig. 3 and Fig. 4. The maximum power at short cavity of the conventional crystal was much lower than that of the other two composite crystals mainly due to the difference in dopant concentration. The critical cavity length is determined based on unified criterion that the output power is dropped to the 70% of maximum power at the stable (short) cavity. The corresponding focal length of thermal lens f_{th} is expressed by [23]

$$\frac{1}{f_{th}} = \frac{1}{d_2 + l \left(\frac{1}{n} - 1 \right)} - \frac{1}{r - d_1} \quad (1)$$

where d_1 and d_2 are the distances from the pumped facet of laser crystal to the front mirror and output coupler, respectively, l is the length of the laser crystal, n is the refractive index of the laser crystal, r is the radius of curvature of the front mirror. d_1 was around 2.4, 1.1, and 1.6 mm for conventional Nd:YVO₄, composite YVO₄-Nd:YVO₄, and YVO₄-Nd:YVO₄-YVO₄, respectively, and was fixed during the experiments. We substitute the critical cavity lengths in terms of d_1 and d_2 into the Eq. (1) to get the effective focal lengths of thermal lens f_{th} . Even though this easy experimental method can not give an absolutely accurate f_{th} , the relative precision is sufficient to make comparison of thermal properties. The experimentally obtained f_{th} are plotted as symbols in Fig. 5. According to the theoretical thermal modeling of CW end-pumped solid-state laser presented by Innocenzi *et al.*, the effective focal length can be approximately expressed by [24]

$$f_{th} = \frac{\pi K \omega_p^2}{\xi P_{in} (dn/dT)} \left[\frac{1}{1 - \exp(-\alpha l_a)} \right] = \frac{C \omega_p^2}{P_{in}} \quad (2)$$

where K is the thermal conductivity, ω_p is the pump-beam radius in the active medium in the unit of mm, ξ is the fractional thermal loading, P_{in} is the pump power in the unit of watt (W), (dn/dT) is the thermal-optical coefficient of n , α is the absorption coefficient, l_a is the length of the active medium, C is a proportional constant in the unit of W/mm. Because the thermal conductivity of YVO₄ in the b- and c-axis of 5.1 and 5.23 W/mK are very close, respectively, it can be seen as a radial symmetry thermal model [4]. The Innocenzi model for rod-type crystal is available here. The Eq. (2) is used to fit the experimental data and the theoretical fitted curves with the approximate corresponding constants C are depicted in Fig. 5.

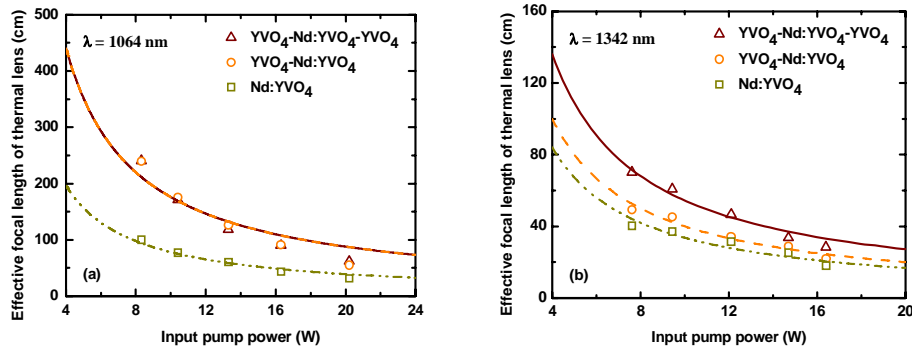


Fig. 5. The relationship between the effective focal length of thermal lens and the input pump power for three types of Nd:YVO₄ crystal operated at (a) 1064 (b) 1342 nm. The symbols represent experimental data and the curves are theoretical fitted results.

The constants C of the conventional Nd:YVO₄, composite YVO₄-Nd:YVO₄, and YVO₄-Nd:YVO₄-YVO₄ for the 1064-nm transition are 4.9×10^4 , 11×10^4 , and 11×10^4 W/mm, respectively. The constants C of the conventional Nd:YVO₄, composite YVO₄-Nd:YVO₄, and YVO₄-Nd:YVO₄-YVO₄ for the 1342-nm transition are 2.1×10^4 , 2.5×10^4 , and 3.4×10^4 W/mm, respectively. The bigger constant C which represents the longer focal length of thermal lens means the weaker thermal lensing effect. The increase of the pump power enhanced the thermal lensing effect. With the equal pump power, the focal length of thermal lens for CW 1342-nm laser was shorter than that for CW 1064-nm laser due to the higher thermal loading.

The higher thermal loading accompanying the lower conversion efficiency was mainly attributed to the higher quantum defect for the longer laser wavelength.

According to the above-mentioned constants C , it is proven that both the focal lengths of thermal lens in the $\text{YVO}_4\text{-Nd:YVO}_4$ and $\text{YVO}_4\text{-Nd:YVO}_4\text{-YVO}_4$ were increased by nearly 2.2-times that in the conventional Nd:YVO_4 for the 1064-nm transition. The focal lengths of thermal lens in the $\text{YVO}_4\text{-Nd:YVO}_4$ and $\text{YVO}_4\text{-Nd:YVO}_4\text{-YVO}_4$ were increased by nearly 1.2 and 1.6-times that in the conventional Nd:YVO_4 for the 1342-nm transition, respectively. Even though the ability of thermal diffusivity in a laser crystal with bigger cross section was inferior [16, 25], the focal lengths of thermal lens in the two composite Nd:YVO_4 crystals were longer than that in the conventional Nd:YVO_4 crystal. In addition, we discuss the influence of different dopant concentration and the length of active medium on the thermal lens. The absorption coefficient α for a typical laser diode with the center wavelength of 808 nm is expressed by [4]

$$\alpha = 2 \cdot N_d \text{ (mm}^{-1}\text{)} \quad (3)$$

where N_d is the Nd dopant concentration in the unit of %. The values of al were 4.86, 5.58, and 5.88 for the conventional Nd:YVO_4 , the composite $\text{YVO}_4\text{-Nd:YVO}_4$, and $\text{YVO}_4\text{-Nd:YVO}_4\text{-YVO}_4$, respectively. According to the Eq. (2), the bigger value of al represents the shorter focal length of thermal lens. But the differences in the value of $[1-\exp(-al)]^{-1}$ between the three crystals was below 0.5 % and could be ignored. Further, the influence of different cross section on the thermal diffusivity was small for edge cooling system. Even we consider the influence, the conventional crystal with small cross section would have better thermal diffusivity and the conclusion does not be changed. Therefore, it is seen that the improvement of thermal lensing effect contributed by employing the two diffusion-bonded Nd:YVO_4 crystals greatly overcame the disadvantage of the bigger cross section.

The experimental results revealed that the thermal lensing effect in the $\text{YVO}_4\text{-Nd:YVO}_4$ was nearly equal to that in the $\text{YVO}_4\text{-Nd:YVO}_4\text{-YVO}_4$ for the highest efficient 1064-nm transition. Therefore only single undoped end at the pumped facet of laser crystal was sufficient for improving the thermal lensing effect to increase the effective focal length of thermal lens to nearly 2.2 times that of the conventional Nd:YVO_4 crystal for CW 1064-nm laser. However, the improvement in thermal lensing effect of the $\text{YVO}_4\text{-Nd:YVO}_4\text{-YVO}_4$ noticeably outperformed that of the $\text{YVO}_4\text{-Nd:YVO}_4$ for the 1342-nm transition. As a result of the stronger thermal lensing effect for the 1342-nm transition, the double undoped ends bonded to the both facets of active medium were essential for assisting thermal diffusing to increase the effective focal length of thermal lens to nearly 1.6 times that of the conventional Nd:YVO_4 crystal.

4. Conclusion

The comparison of thermal lensing effects between diffusion-bonded $\text{YVO}_4\text{-Nd:YVO}_4$ and $\text{YVO}_4\text{-Nd:YVO}_4\text{-YVO}_4$ crystals with single- and double-end, respectively, was demonstrated by measuring the effective focal lengths of thermal lens. The both types of diffusion-bonded crystal could improve the thermal lensing effects of conventional Nd:YVO_4 crystal. The $\text{YVO}_4\text{-Nd:YVO}_4$ was capable of accomplishing the improvement in thermal lensing effect of $\text{YVO}_4\text{-Nd:YVO}_4\text{-YVO}_4$ for the 1064-nm transition. However, the improvement of $\text{YVO}_4\text{-Nd:YVO}_4\text{-YVO}_4$ remarkably towered over that of $\text{YVO}_4\text{-Nd:YVO}_4$ for the 1342-nm transition with stronger thermal lensing effect. Therefore $\text{YVO}_4\text{-Nd:YVO}_4$ and $\text{YVO}_4\text{-Nd:YVO}_4\text{-YVO}_4$ crystals can serve as promising substitutes for a conventional Nd:YVO_4 crystal to reduce thermal lensing effect and scale to a higher average power of diode-end-pumped CW Nd:YVO_4 lasers operated at 1064 and 1342 nm, respectively.

Acknowledgments

The authors thank the National Science Council for their financial support of this research under Contract No. NSC-95-2112-M-009-041-MY2.